Protein kinase C mediates the phosphorylation of the Nem1–Spo7 protein phosphatase complex in yeast

Received for publication, August 9, 2019, and in revised form, September 4, 2019 Published, Papers in Press, September 9, 2019, DOI 10.1074/jbc.RA119.010592

Prabuddha Dey, Wen-Min Su, Mona Mirheydari, Gil-Soo Han, and George M. Carman[1]

From the Department of Food Science and the Rutgers Center for Lipid Research, New Jersey Institute for Food, Nutrition, and Health, Rutgers University, New Brunswick, New Jersey 08901

Edited by Dennis R. Voelker

The Nem1–Spo7 complex in the yeast *Saccharomyces cerevisiae* is a protein phosphatase required for the nuclear/endoplasmic reticulum membrane localization of Pah1, a phosphatidate phosphatase that produces diacylglycerol for triacylglycerol synthesis at the expense of phospholipid synthesis. In a previous study, we showed that the protein phosphatase is subject to phosphorylation by protein kinase A (PKA). Here, we demonstrate that Nem1–Spo7 is regulated through its phosphorylation by protein kinase C (PKC), which plays multiple roles, including the regulation of lipid synthesis and cell wall integrity. Phosphorylation analyses of Nem1–Spo7 and its synthetic peptides indicate that both subunits of the complex are *bona fide* PKC substrates. Site-directed mutagenesis of *NEM1* and *SPO7*, coupled with phosphopeptide mapping and immunoblotting with a phosphoserine-specific PKC substrate antibody, revealed that Ser-201 in Nem1 and Ser-22/Ser-28 in Spo7 are major PKC target sites of phosphorylation. Activity analysis of mutant Nem1–Spo7 complexes indicates that the PKC phosphorylation of Nem1 exerts a stimulatory effect, but the phosphorylation of Spo7 has no effect. Lipid-labeling analysis of cells expressing the phosphorylation-deficient alleles of *NEM1* and *SPO7* indicates that the stimulation of the Nem1–Spo7 activity has the effect of increasing triacylglycerol synthesis. Prephosphorylation of Nem1–Spo7 by PKC inhibits the PKA phosphorylation of Nem1, whereas prephosphorylation of the phosphatase complex by PKA inhibits the PKC phosphorylation of Spo7. Collectively, this work advances the understanding of the Nem1–Spo7 regulation by phosphorylation and its impact on lipid synthesis.

The *PAH1*-encoded PA[2] phosphatase (Pah1) (1), which catalyzes the dephosphorylation of PA to yield DAG (2), has emerged as a key regulatory enzyme in yeast[3] that controls the bifurcation of PA between DAG and CDP-DAG (3–7) (see Fig. 1*A*). Elevated PA phosphatase activity is associated with the production of DAG that is used for the synthesis of the storage lipid TAG, whereas reduced enzyme activity is associated with the production of CDP-DAG that is used for the synthesis of membrane phospholipids (3–7). In yeast, the PA-derived synthesis of membrane phospholipids predominates over the synthesis of TAG during logarithmic growth, but as cells enter the stationary phase of growth, the PA is primarily partitioned into TAG (3, 5–7). The Pah1 PA phosphatase is the primary regulator of this metabolic switch (3, 5–7).

Loss of PA phosphatase activity, as exemplified by the *pah1*Δ mutation, has devastating effects on lipid metabolism and cell physiology (7). Lack of DAG production reduces TAG synthesis and lipid droplet formation (8). Consequently, fatty acids accumulate (1), rendering the mutant cells susceptible to fatty acid–induced lipotoxicity (1, 9). PA accumulates at the nuclear/ER membrane (10), which drives the synthesis of membrane phospholipids via CDP-DAG by mass action and by the PA/Opi1-mediated derepression of phospholipid synthesis genes (1, 9, 11–13). The notable *pah1*Δ phenotype is an aberrant nuclear morphology with the expansion of the nuclear/ER membrane (11). Moreover, the mutant cells have fragmented vacuoles (14) and a weakened cell wall (15, 16). They are also hypersensitive to hydrogen peroxide (17), do not grow on glycerol (nonfermentable carbon source) (1, 18), are sensitive to heat (1, 11, 19, 20) and cold (21), exhibit a defect in autophagy induction after TORC1 inactivation (22), have a shortened chronological life span (17), and exhibit apoptotic cell death in the stationary phase (9).

As one might expect, the function of such an important regulatory enzyme is controlled by genetic and biochemical mechanisms, with perhaps phosphorylation and dephosphorylation being the most important (3, 5–7). These posttranslational modifications control the location and stability of Pah1 as well as its PA phosphatase activity (23–33). In general, the phosphorylation on multiple sites, as mediated by several protein kinases (*e.g.* Cdc28-cyclin B, Pho85-Pho80, and PKA), attenuates enzyme function by sequestering Pah1 in the cytosol apart from its membrane-associated substrate PA and by inhibiting the PA phosphatase activity. The dephosphorylation of Pah1, as mediated by the Nem1 (catalytic)–Spo7 (regulatory) protein phos-

This work was supported by National Institutes of Health Grant GM050679 from the United States Public Health Service. The authors declare that they have no conflicts of interest with the contents of this article. The content is solely the responsibility of the authors and does not necessarily represent the official views of the National Institutes of Health.

[1] To whom correspondence should be addressed: Dept. of Food Science, Rutgers University, 61 Dudley Rd., New Brunswick, NJ 08901. Tel.: 848-932-0267; E-mail: gcarman@rutgers.edu.

[2] The abbreviations used are: PA, phosphatidic acid; DAG, diacylglycerol; ER, endoplasmic reticulum; PKA, protein kinase A, PKC, protein kinase C; PS, phosphatidylserine; PVDF, polyvinylidene difluoride; TAG, triacylglycerol; CTDNEP1, C-terminal domain nuclear envelope phosphatase 1; NEP1-R1, nuclear envelope phosphatase 1–regulatory subunit 1; TM, transmembrane.

[3] In this paper, yeast is used interchangeably with *S. cerevisiae*.

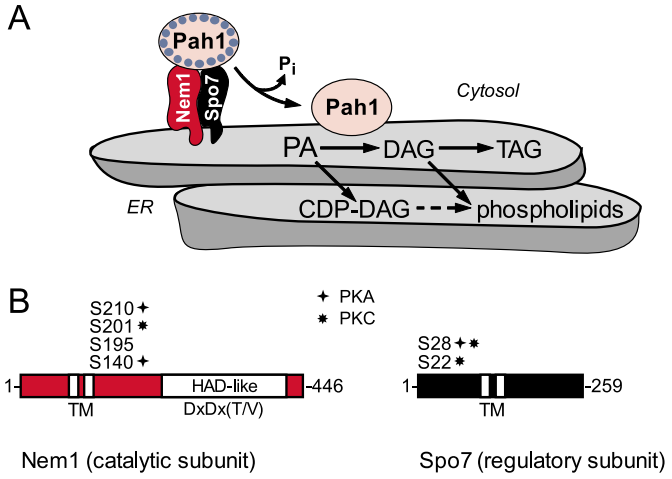

Figure 1. Reactions catalyzed by the Nem1–Spo7 phosphatase complex and the Pah1 PA phosphatase and their roles in lipid synthesis; domains/regions and phosphorylation sites in Nem1 and Spo7. *A*, phosphorylated (indicated by *small circles*) Pah1 interacts with the Nem1–Spo7 complex at the ER membrane. Following its dephosphorylation, Pah1 that is associated with the ER membrane dephosphorylates PA to produce DAG. The DAG produced by the PA phosphatase reaction is used for the synthesis of TAG. PA is also utilized for the synthesis of membrane phospholipids via CDP-DAG. When the CDP-DAG–dependent pathway for phospholipid synthesis is blocked, phosphatidylcholine or phosphatidylethanolamine, respectively, may be synthesized from the DAG derived from the PA phosphatase reaction when cells are supplemented with choline or ethanolamine, respectively, via the CDP-choline or CDP-ethanolamine branches of the Kennedy pathway. Details of the lipid synthesis pathways may be found elsewhere (95, 96). *B*, Nem1 and Spo7 are integral nuclear/ER membrane proteins possessing two transmembrane (TM)-spanning domains (34). Nem1 binds to Spo7 through its conserved C-terminal domain, and this association is responsible for the formation of the complex (34). Nem1, which serves as the catalytic subunit, is a member of the haloacid dehalogenase superfamily (97, 98); its phosphatase activity is conferred by the D*X*D*X*(T/V) catalytic motif within its haloacid dehalogenase (*HAD*)-like domain (11, 34). Spo7, which serves as the regulatory subunit (34), facilitates the formation of the Nem1–Spo7/Pah1 complex (31, 38).

phatase complex, has the opposite effects (23–30, 33). Paradoxically, the phosphorylation stabilizes Pah1 abundance, whereas the dephosphorylation promotes degradation via the 20S proteasome (32, 33). An exception to this situation is that phosphorylation by PKC, when not already phosphorylated by Pho85–Pho80, stimulates the 20S proteasome–mediated degradation of Pah1 (27).

The Nem1–Spo7 phosphatase complex (34) is a major regulator of Pah1 function; it is responsible for recruiting and dephosphorylating Pah1 at the ER membrane and for stimulating PA phosphatase activity (23, 30, 31) (Fig. 1). Given the function of Nem1–Spo7 to activate Pah1, it is not surprising that the *nem1*Δ and/or *spo7*Δ mutant exhibits the same phenotypes as those of the *pah1*Δ mutant (11, 12, 22, 34,35). Whereas the phosphatase complex functions to dephosphorylate Pah1, both Nem1 and Spo7 are also subject to phosphorylation (36–40) (Fig. 1*B*). In the current work, we characterized the phosphorylation of Nem1–Spo7 complex by PKC, a PS/DAG-dependent protein kinase in yeast (39) that is required for cell cycle progression (41) and plays a role in regulating lipid synthesis (42–47) and in maintaining cell wall integrity (41, 48, 49). Ser-201 in Nem1 and Ser-22/Ser-28 in Spo7 were identified as the principal sites of phosphorylation. Lipid composition analysis of cells bearing phosphorylation-site mutations indicated that PKC has a positive impact on fine-tuning TAG synthesis through the phosphorylation and stimulation of Nem1–Spo7 phosphatase activity.

Results

PKC phosphorylates Nem1 and Spo7

In the previous work, we demonstrated that *Saccharomyces cerevisiae* PKC phosphorylates the *Escherichia coli*–expressed Nem1-ΔTM and Spo7-ΔTM and that these phosphorylations require PS and DAG (39). In the current work, we further characterized the PKC-mediated phosphorylations of Nem1 and Spo7 using full-length proteins expressed and purified as a complex from *S. cerevisiae*. As described previously (40), we expressed Nem1 as a fusion protein tagged with protein A to facilitate its purification by affinity chromatography with IgG-Sepharose (34). The purified Nem1–Spo7 complex was nearly homogeneous and enzymatically active for the dephosphorylation of Pah1 phosphorylated by Pho85–Pho80 (29). The Nem1–Spo7 complex was incubated with PKC and [γ-^{32}P]ATP followed by the separation of the phosphorylated products from ATP by SDS-PAGE and then subjected to phosphorimaging analysis. The phosphorimage shown in Fig. 2*A* (*left*) demonstrates that PKC phosphorylated both Nem1 and Spo7. The immunoblot analysis with the anti-Nem1 and anti-Spo7 antibodies confirmed that Nem1 and Spo7 are phosphorylated by PKC (Fig. 2*A*, *right*). The phosphoamino acid analysis of the ^{32}P-labeled proteins showed that Nem1 and Spo7 are phosphorylated on both serine and threonine residues with serine being the major target of phosphorylation (Fig. 2*B*). The phosphopeptide mapping analysis showed one major phosphopeptide from ^{32}P-labeled Nem1 and three major phosphopeptides from ^{32}P-labeled Spo7 (Fig. 2*C*). The radioactive label in the Nem1 phosphopeptide was attributed to the phosphorylation of Ser-201, whereas the label in the Spo7 phosphopeptides was attributed to the phosphorylations of Ser-22 and Ser-28 (see below).

The PKC-mediated phosphorylation of Nem1 and Spo7 was examined with respect to the time of the reaction, the amount of PKC used in the reaction, and the ATP concentration (Fig. 3). The stoichiometry for each reaction was consistent with the conclusion that Nem1 and Spo7 have at least one PKC phosphorylation site. That the stoichiometry of the reactions was less than a theoretical value of 1 (for Nem1) and 2 (for Spo7) indicated that some Nem1 and Spo7 molecules are endogenously phosphorylated by PKC. These data also indicated that PKC phosphorylates Spo7 to a greater extent when compared with Nem1. That the phosphorylation reactions were dependent on time (Fig. 3*A*) and the amount of protein kinase (Fig. 3*B*) indicated that PKC activity followed zero-order kinetics using Nem1 and Spo7 as substrates. Additionally, the PKC activity toward Nem1 (K_m = 10.5 μM) and Spo7 (K_m = 12.1 μM) followed saturation kinetics with respect to the ATP concentration; the apparent Michaelis constants for ATP of both substrates were similar (Fig. 3*C*). We did not conduct a kinetic analysis of PKC activity with respect to Nem1 and Spo7 because of a limitation in the amount of pure Nem1–Spo7 complex.

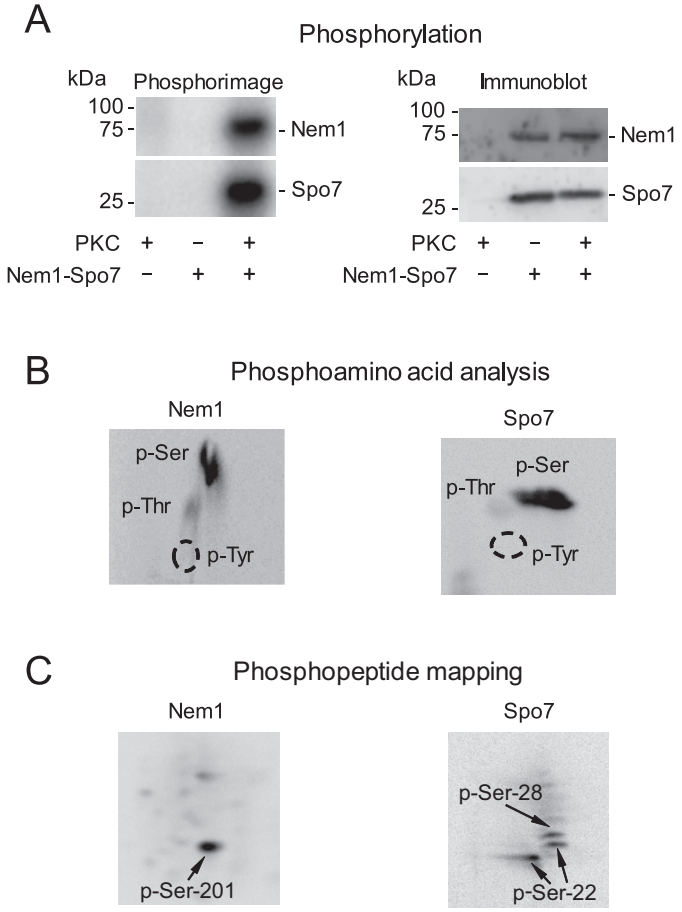

Figure 2. Nem1 and Spo7 are majorly phosphorylated *in vitro* by PKC on the serine residue; Ser-201 in Nem1 and Ser-22 and Ser-28 in Spo7 are the major PKC phosphorylation sites. The protein A–tagged Nem1 was coexpressed with Spo7 in yeast cells, and the Nem1–Spo7 complex was purified by IgG-Sepharose affinity chromatography. The complex (40 ng) was incubated at 30 °C for 20 min with 70 ng of PKC, 40 μM [γ-^{32}P]ATP, 10 mM $MgCl_2$, 500 μM PS, 150 μM DAG, and 1.7 mM $CaCl_2$. The reaction mixture was resolved by SDS-PAGE. *A*, the radioactive phosphorylations of Nem1 and Spo7 were visualized by phosphorimaging of the SDS-polyacrylamide gel (*left*). The proteins were transferred to a PVDF membrane, which was split into the upper and lower portions and used for immunoblot analysis using anti-Nem1 and anti-Spo7 antibodies, respectively (*right*). The positions of Nem1, Spo7, and molecular mass standards are indicated. *B*, PVDF membrane containing ^{32}P-labeled Nem1 or Spo7 was incubated with 6 N HCl for 90 min at 110 °C. The acid hydrolysates were separated by two-dimensional electrophoresis on cellulose TLC plates followed by phosphorimaging analysis. The positions of the standard phosphoamino acids phosphoserine (*p-Ser*), phosphothreonine (*p-Thr*), and phosphotyrosine (*p-Tyr*) (*dotted lines*) are indicated. *C*, PVDF membrane containing ^{32}P-labeled Nem1 or Spo7 was digested with L-1-tosylamido-2-phenylethyl chloromethyl ketone–treated trypsin. The phosphopeptides produced by the proteolytic digestion were separated on cellulose TLC plates by electrophoresis (from *left* to *right*) in the first dimension and by chromatography (from *bottom* to *top*) in the second dimension. The identity of the phosphorylation sites in the radioactive phosphopeptides of Nem1 or Spo7 was determined from phosphopeptide maps of the phosphorylation-deficient alanine mutations of Ser-201 of Nem1 and Ser-22 and Ser-28 of Spo7. The data shown in *A–C* are representative of three independent experiments.

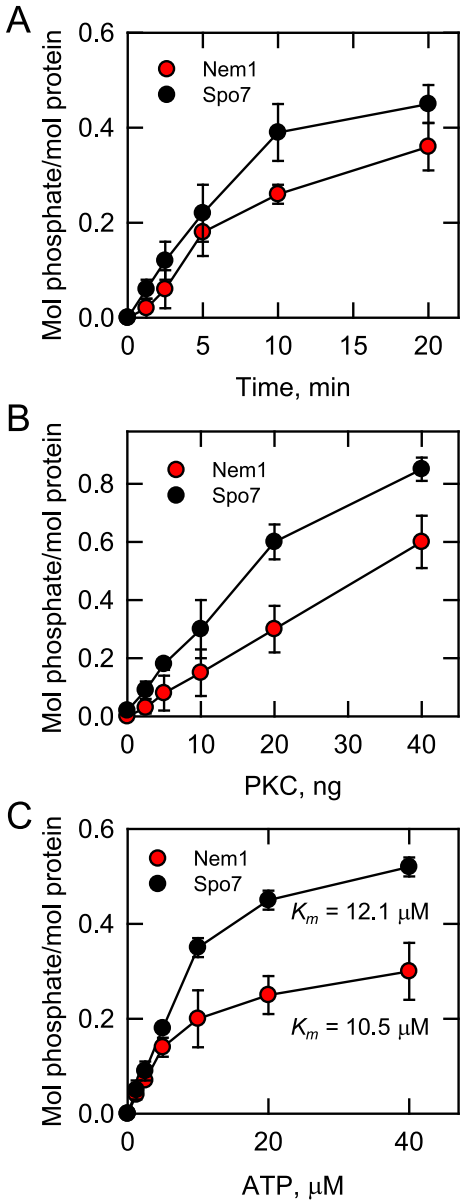

Figure 3. Phosphorylations of Nem1 and Spo7 by PKC are dependent on time, the amount of PKC, and ATP concentration. Purified Nem1–Spo7 complex (40 ng) was phosphorylated by PKC using [γ-^{32}P]ATP as described in the legend to Fig. 2. The PKC reaction was conducted by varying the reaction time (*A*), amount of PKC (*B*), and concentration of ATP (*C*). *A* and *B*, 40 μM ATP; *A* and *C*, 20 ng of PKC; *B* and *C*, 15 min. The amount of radioactive phosphate incorporated into Nem1 or Spo7 was determined from a standard curve using [γ-^{32}P]ATP. The amounts of Nem1 and Spo7 were determined by comparing their band intensities from a SYPRO Ruby–stained polyacrylamide gel with a standard curve of BSA. The data shown are averages of three experiments ±S.D. (*error bars*).

PKC phosphorylates Ser-201 in Nem1 and Ser-22/Ser-28 in Spo7 in vitro and in vivo

We used a multifaceted approach to identify major PKC phosphorylation sites in the Nem1-Spo7 subunits. The NetPhosK (50) and NetPhosYeast (51) algorithms predict PKC phosphorylation sites in the cytosol-facing regions of Nem1 or Spo7. Peptides containing the putative phosphorylation sites were synthesized and tested as substrates for the protein kinase (Fig. 4). The Nem1 peptide corresponding to residues 191–205 was majorly phosphorylated. Within this sequence are the putative PKC target sites of Ser-195, Ser-201, and Ser-204. The mutation of Ser-195, a site previously shown to be phosphorylated in response to rapamycin treatment (38), to a nonphosphorylatable alanine residue did not affect the phosphorylation by PKC. Thus, by this assay, Ser-195 is not a PKC target site. To test the hypothesis that Ser-201 and Ser-204 are the PKC sites of phos-

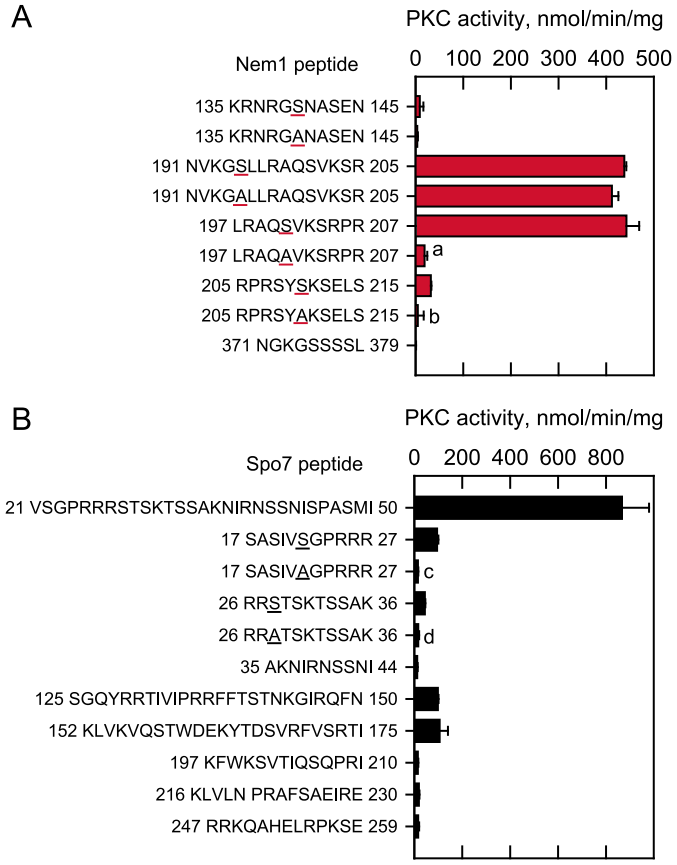

Figure 4. PKC phosphorylates Nem1 or Spo7 synthetic peptides that contain sites of phosphorylation. PKC activity was measured with a 100 μM concentration of the indicated Nem1 (*A*) or Spo7 (*B*) peptides at 100 μM [γ-^{32}P]ATP. The enzyme reaction, which was performed without PS, DAG, or $CaCl_2$, was terminated by spotting the mixture onto a P81 phosphocellulose paper, which was then washed with 75 mM phosphoric acid and subjected to scintillation counting. The *numbers* at the beginning and end of the Nem1 (*A*) and Spo7 (*B*) peptides represent the positions in the full-length sequences of the respective proteins. The *underlined* residues within the Nem1 and Spo7 peptides designate the serine-to-alanine substitutions in the sequence. The data are the averages of three experiments ± S.D. (*error bars*). *a*, $p < 0.05$ *versus* WT peptide, residues 197–207; *b*, $p < 0.05$ *versus* WT peptide, residues 205–215; *c*, $p < 0.05$ *versus* WT peptide, residues 17–27; *d*, $p < 0.05$ *versus* WT peptide, residues 26–36.

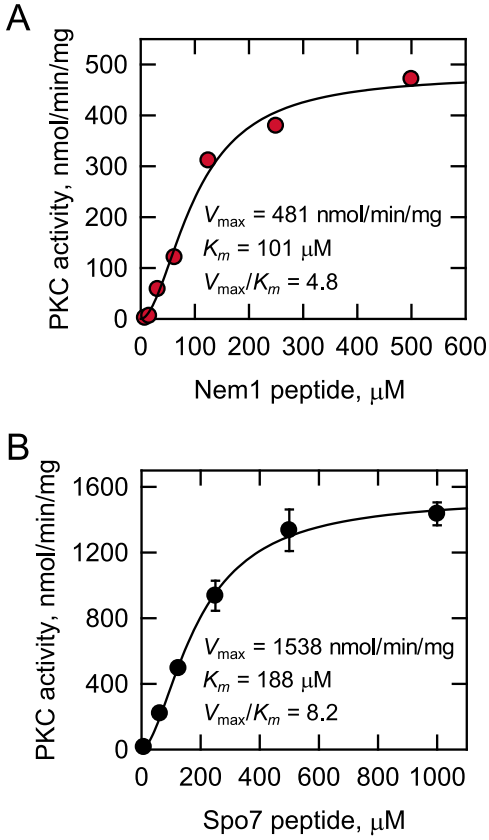

Figure 5. Kinetics of PKC activity on Nem1 and Spo7 synthetic peptides. PKC activity was measured as a function of the concentrations of the Nem1 peptide (residues 197–207) (*A*) or the Spo7 peptide (residues 21–50) (*B*) at 1 mM [γ-^{32}P]ATP. The enzyme reaction, which was performed without PS, DAG, or $CaCl_2$, was terminated by spotting the mixture onto P81 phosphocellulose paper, which was then washed with 75 mM phosphoric acid and subjected to scintillation counting. The apparent V_{max} and K_m values were determined by analysis of the data with the Enzyme Kinetics module of SigmaPlot software according to the Michaelis–Menten equation. The data are averages of three experiments ±S.D. (*error bars*).

phorylation, the peptide corresponding to residues 197–207 was synthesized and used for the assay of PKC activity. This peptide was a good substrate of PKC, but when alanine was substituted for serine at position 201, the activity was reduced by 96% (Fig. 4*A*). This result supported the notion that Ser-201 is a major site of phosphorylation by PKC. If Ser-204 is a site of phosphorylation, it is a minor site. We also examined the PKC activity using the synthetic peptide of Nem1 residues 205–215. Among the serine residues in this peptide is Ser-210, previously identified as a major target site for PKA phosphorylation (40). The peptide was phosphorylated by PKC, and the alanine mutation of serine at position 210 reduced the activity by 85% (Fig. 4*A*). However, the PKC activity on the WT peptide of residues 205–215 was only 7% of the activity on the peptide of residues 197–207. Thus, we concluded that Ser-210, as well as the other serine residues (*e.g.* Ser-208, Ser-212, and Ser-215), are not major sites of phosphorylation by PKC.

Peptides were synthesized that cover the soluble regions of Spo7, and we examined them for their phosphorylation by PKC (Fig. 4*B*). The Spo7 peptide of residues 21–50 was a PKC substrate. Shorter Spo7 peptides that contain Ser-22 (residues 17–27) and Ser-28 (residues 26–36) also served as substrates, but the kinase activity on these peptides was 10–20-fold lower when compared with the longer peptide (residues 21–50). Nonetheless, the alanine mutations of the short peptides at residues 22 and 28 reduced the PKC activity by 85 and 64%, respectively. The Spo7 peptides of residues 125–150 and residues 152–175 were relatively poor PKC substrates when compared with the peptide of residues 21–50. Accordingly, the identification of the residues being phosphorylated in these peptides was not pursued.

We performed a kinetic analysis of PKC activity on the Nem1 peptide (residues 197–207) and the Spo7 peptide (residues 21–50). In these experiments, the PKC activity on each peptide was measured with various peptide concentrations at the saturating concentration of ATP. The specificity constant, V_{max}/K_m (52), for the Spo7 peptide is 1.7-fold higher than that of the Nem1 peptide (Fig. 5), and thus, the Spo7 peptide is the better substrate.

To further confirm that Ser-201 in Nem1 and Ser-22/Ser-28 in Spo7 are target sites of PKC phosphorylation, the alanine mutations of these serine residues were constructed in the full-length genes. The phosphorylation-deficient mutant forms of

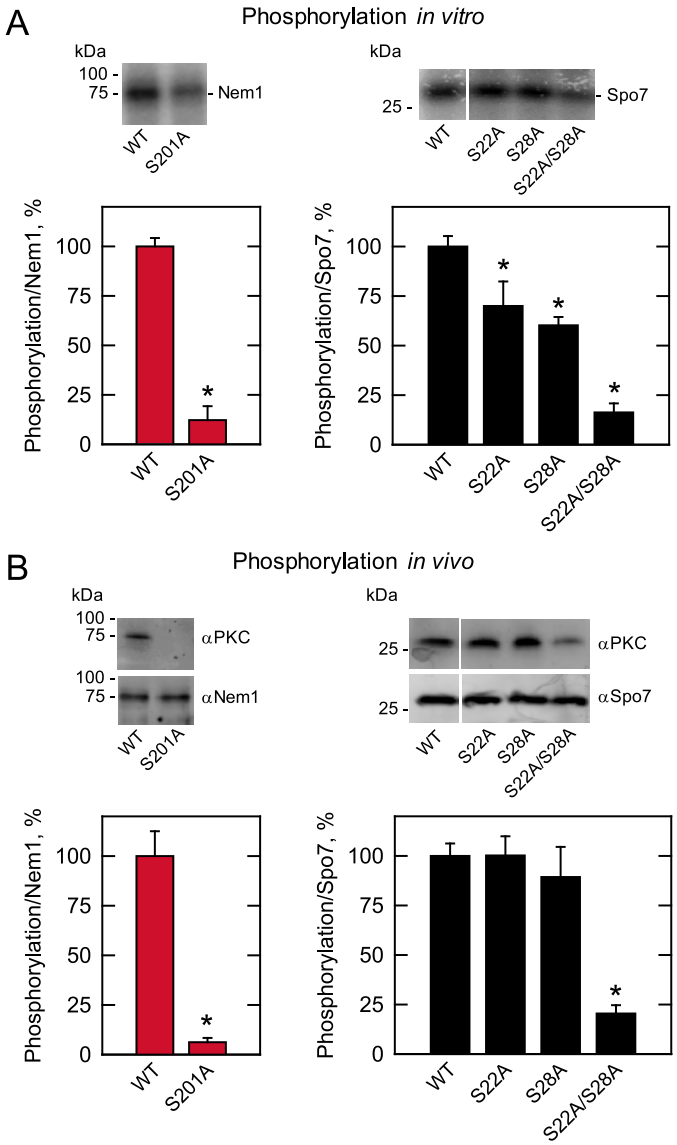

Figure 6. Alanine mutations of Ser-201 in Nem1 and Ser-22/Ser-28 in Spo7, respectively, reduce their phosphorylations by PKC *in vitro* and *in vivo*. The WT and indicated mutant forms of Nem1 or Spo7 were coexpressed in yeast cells and purified by IgG-Sepharose affinity chromatography based on the protein A tag on Nem1. *A*, the purified Nem1–Spo7 complex (40 ng) was phosphorylated by PKC (40 ng) with [γ-^{32}P]ATP (40 μM) as described in the legend to Fig. 2. Following the reaction, samples were subjected to SDS-PAGE. The phosphorylations of Nem1 and Spo7 were visualized by phosphorimaging. The proteins on the gel were visualized with SYPRO Ruby stain (not shown). *B*, the purified Nem1–Spo7 complex (20 ng) was subjected to SDS-PAGE followed by transfer to a PVDF membrane and probing with anti-phosphoserine PKC substrate antibody. A duplicate PVDF membrane was split into the upper and lower portions and used for immunoblot analysis with anti-Nem1 and anti-Spo7 antibodies, respectively. The phosphorimages, SYPRO Ruby–stained polyacrylamide gels, and immunoblots were quantified by ImageQuant analysis. The positions of Nem1, Spo7, and molecular mass standards are indicated. The PKC-mediated phosphorylation levels of the mutant proteins were compared with the respective WT proteins that were set at 100%. The phosphorimages (*A*) and immunoblots (*B*) are representative of three experiments, whereas the quantification data shown below the images are averages of three experiments ±S.D. (*error bars*). *, $p < 0.05$ *versus* WT.

Nem1 (tagged with protein A for purification of the complex) and Spo7 were coexpressed and purified as a complex from *S. cerevisiae* cells. In the PKC phosphorylation of Nem1 *in vitro*, the S201A mutation caused an 88% reduction in the extent of phosphorylation (Fig. 6*A*, *left*). The phosphorylated S201A mutant protein was subjected to two-dimensional phosphopeptide mapping analysis. The major phosphopeptide labeled as p-Ser-201 in the map of the WT Nem1 (Fig. 2*C*, *left*) was eliminated in the map of the S201A mutant protein, confirming that Ser-201 is the major site of phosphorylation by PKC *in vitro*. To confirm that the S201A mutation affects the phosphorylation of Nem1 *in vivo*, the WT and mutant proteins expressed and purified from yeast were examined by immunoblotting with an antibody directed against the phosphoserine PKC substrate. The immunodetection of the WT Nem1 with the antibody showed that the protein is endogenously phosphorylated by PKC (Fig. 6*B*, *left*). The S201A mutation caused a 96% reduction in the amount of Nem1 detected by the antibody.

In the PKC phosphorylation of Spo7 *in vitro*, the S22A, S28A, and S22A/S28A mutations had the effects of 30, 40, and 84% reductions in the extent of phosphorylation when compared with the WT control (Fig. 6*A*, *right*). Each of the phosphorylated mutant proteins was subjected to the phosphopeptide mapping analysis. The two phosphopeptides labeled as p-Ser-22 and the one phosphopeptide labeled as p-Ser-28 in the phosphopeptide map of the WT Spo7 protein (Fig. 2*C*, *right*) were not detected from the phosphopeptide maps of the S22A and S28A mutants, respectively. The anti-phosphoserine PKC substrate antibody was also used to assess the effects of the phosphorylation-deficient alanine mutations on the endogenous phosphorylation of Spo7 by PKC (Fig. 6*B*, *right*). The antibody recognized WT Spo7, confirming that the protein is phosphorylated by PKC *in vivo*. Individually, the S22A and S28A mutations did not have a significant effect on the endogenous phosphorylation of Spo7 by PKC. However, the S22A/S28A double mutation caused an 80% reduction in the phosphorylation of Spo7 by PKC *in vivo* (Fig. 6*B*, *right*).

The S201A mutation in Nem1 reduces Nem1–Spo7 phosphatase activity

The effect of Nem1–Spo7 phosphorylation by PKC on the protein phosphatase activity was examined as a function of time. The phosphorylation of the Nem1–Spo7 complex had a small stimulatory effect on the activity (Fig. 7*A*). We considered that the effect of the phosphorylation on the phosphatase activity was dampened by the phosphorylation state of the complex. As indicated above, the isolated complex is subject to endogenous phosphorylation. As described previously (40), treatment of the purified complex with alkaline phosphatase reduced its phosphatase activity by 58%. Subsequent phosphorylation of the complex by PKC did not have a significant effect on Nem1–Spo7 phosphatase activity. The purified complex, with the S201A mutation in Nem1 or the S22A/S28A mutations in Spo7, was examined for the Nem1–Spo7 phosphatase activity. The activity of the complex bearing the mutation in Nem1 was reduced by 53% when compared with the control complex (Fig. 7*B*). The mutations in Spo7 did not affect the Nem1–Spo7 phosphatase activity.

Effects of the PKC phosphorylation–deficient mutations of Nem1 and Spo7 on growth at elevated temperature and on lipid composition

Cells lacking Nem1 (*e.g. nem1*Δ mutant) or Spo7 (*e.g. spo7*Δ mutant) exhibit a temperature-sensitive phenotype (Fig. 8*A*)

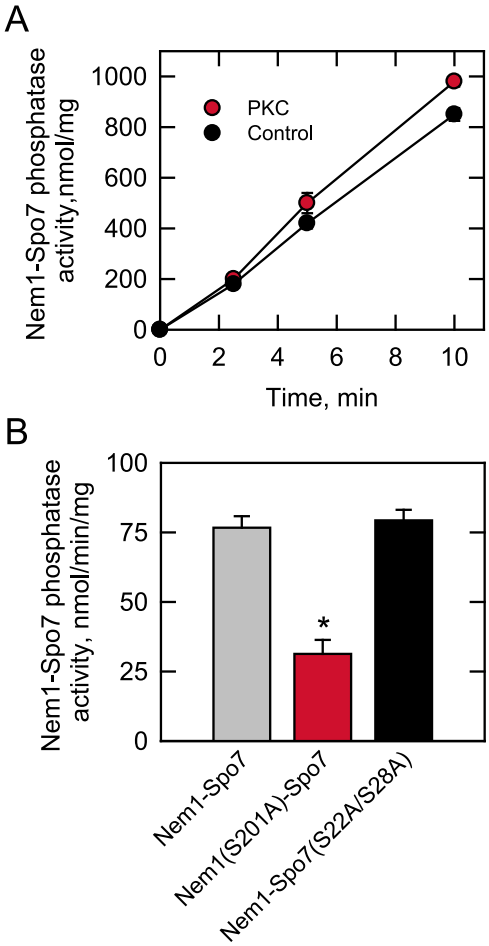

Figure 7. Effects of PKC-mediated phosphorylation and PKC phosphorylation-site mutations on Nem1–Spo7 phosphatase activity. The WT and PKC phosphorylation-site mutant forms of the Nem1–Spo7 complex were expressed and purified from yeast. *A*, 10 ng of the WT Nem1–Spo7 complex was phosphorylated by 40 ng of PKC with unlabeled ATP for 15 min. The PKC-phosphorylated and unphosphorylated (*control*) forms of the complex were assayed for Nem1–Spo7 phosphatase activity for the indicated time intervals. *B*, 10 ng of the WT and the indicated mutant forms of the Nem1–Spo7 complex were assayed for their phosphatase activity for 10 min. Nem1–Spo7phosphatase activity was measured by following the release of $^{32}P_i$ from [^{32}P]Pah1 that was phosphorylated by the Pho85–Pho80 protein kinase. The data shown are means ± S.D. (*error bars*) from triplicate assays. *, $p < 0.05$ *versus* the WT Nem1–Spo7 complex.

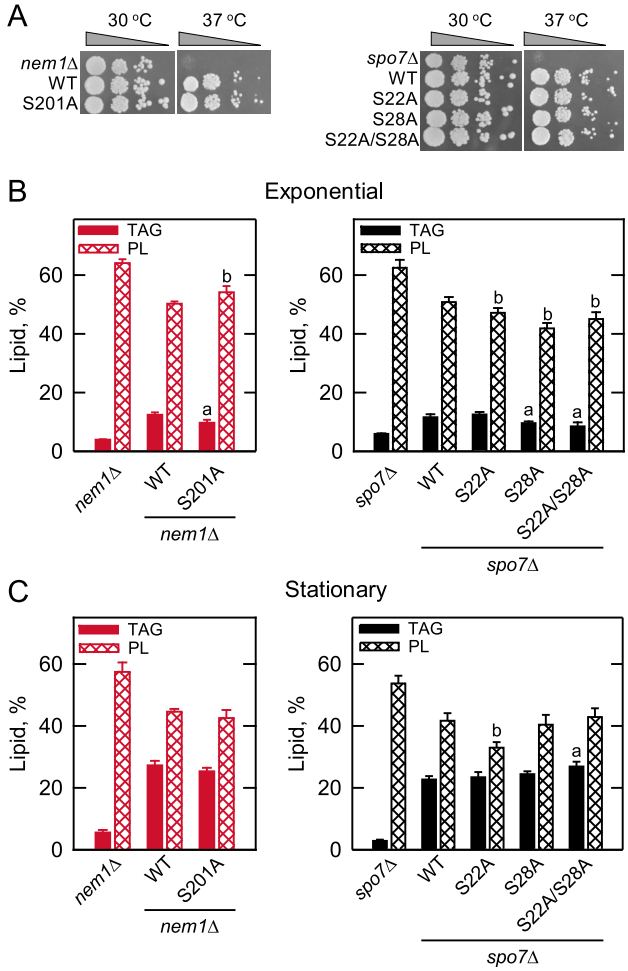

Figure 8. Effects of the PKC phosphorylation-site mutations in Nem1 and Spo7, respectively, on the complementation of the *nem1*Δ or *spo7*Δ temperature-sensitive and the aberrant lipid composition phenotypes. The indicated WT and phosphorylation-deficient forms of Nem1 and Spo7 were expressed in the *nem1*Δ and *spo7*Δ mutants, respectively, and grown in liquid synthetic complete-Leu medium. *A*, saturated cultures were diluted to a density of 0.67 at $A_{600\ nm}$ followed by 10-fold serial dilutions. The diluted cultures were spotted (2.5 μl) onto agar plates and incubated for 5 days at 30 and 37 °C. *B* and *C*, the cells were grown at 30 °C to the exponential (*B*) and stationary (*C*) phases of growth in synthetic complete-Leu medium containing [2-^{14}C]acetate (1 μCi/ml). The lipids were extracted and separated by one-dimensional TLC, and the phosphorimages were subjected to ImageQuant analysis. The percentages shown for TAG and phospholipids (*PL*) were normalized to the total ^{14}C-labeled chloroform-soluble fraction. Each data point represents the average of three experiments ±S.D. (*error bars*). *a*, $p < 0.05$ *versus* TAG of WT; *b*, $p < 0.05$ *versus* phospholipid of WT.

(34), which exemplifies the importance of the Nem1–Spo7 complex in regulating the phosphorylation state of Pah1 (4, 7). The inability of the *nem1*Δ and *spo7*Δ mutant to grow at 37 °C was complemented by the introduction of the *NEM1* and *SPO7* genes, respectively, on a single-copy plasmid into the respective mutant (Fig. 8*A*). The genes containing the PKC phosphorylation-site mutant alleles of *NEM1*(S201A) and *SPO7*(S22A, S28A, and S22A/S28A) were introduced into the *nem1*Δ and *spo7*Δ mutant cells, respectively. The expression of the phosphorylation-deficient form of Nem1 or Spo7 afforded growth at the restrictive temperature (Fig. 8*A*). Thus, the PKC phosphorylation-site mutations of Nem1 and Spo7 do not compromise the function of the Nem1–Spo7 complex at 37 °C.

We considered that the temperature-sensitivity assay was not sufficiently sensitive to reveal the partial loss-of-function effects of the phosphorylation-deficient mutations in Nem1 or Spo7 on the *in vivo* function of the phosphatase complex. Because Nem1–Spo7 is a major regulator of Pah1 function in the synthesis of TAG and phospholipids (4, 53), the effects of the PKC phosphorylation-site mutations in Nem1 and Spo7 on the relative amounts of these lipids were examined (Fig. 8, *B* and *C*). When compared with *nem1*Δ cells expressing the WT *NEM1* gene, those bearing empty plasmid exhibited decreases (70 and 80%, respectively) in the amounts of TAG in the exponential and stationary phases of growth. Also, the *nem1*Δ cells with empty vector exhibited 28 and 29% increases in the relative amounts of phospholipids in the exponential and stationary phases, respectively, when compared with *nem1*Δ cells expressing WT *NEM1*. In the exponential phase, the S201A mutation in Nem1 caused a 28% decrease in TAG and a 7% increase in phospholipids when compared with the lipids of cells expressing the WT

NEM1 gene (Fig. 8*B*, *left*). The S201A mutation did not have a significant effect on the relative amounts of these lipids in the stationary phase (Fig. 8*C*, *left*).

Similar to that observed from *nem1*Δ mutant cells, the *spo7*Δ mutation caused 50 and 88% decreases in the relative amounts of TAG in the exponential and stationary phases, respectively, when compared with those expressing the WT *SPO7* gene (Fig. 8, *B* and *C*, *right*). Additionally, the *spo7*Δ cells exhibited 23 and 29% increases in the levels of phospholipids in the exponential and stationary phases, respectively. In the exponential phase, the relative amounts of TAG in *spo7*Δ cells bearing the S28A and S22A/S28A alleles were 17 and 27% lower, respectively, when compared with those expressing the WT *SPO7*. The relative amounts of phospholipids in the S28A and S22A/S28A cells were reduced by 20 and 12%, respectively. TAG and phospholipids were not affected by the S22A mutation in the exponential-phase cells. However, in the stationary phase, the S22A mutation caused a 21% decrease in phospholipids, and the S22A/S28A double mutation caused an 18% increase in TAG (Fig. 8*C*, *right*).

Prephosphorylation of the Nem1–Spo7 complex by PKC inhibits the PKA phosphorylation of Nem1, and prephosphorylation of the phosphatase complex by PKA inhibits the PKC phosphorylation of Spo7

Because Nem1-Spo7 is also phosphorylated by PKA (40), we questioned what effect the phosphorylation by PKC would have on the phosphorylation by PKA and vice versa. To address this question, the Nem1–Spo7 complex was prephosphorylated by PKC with unlabeled ATP and subsequently phosphorylated by PKA with [γ-^{32}P]ATP (Fig. 9*A*). PKC mediated a dose-dependent reduction (85%) of Nem1 phosphorylation by PKA. The PKA-mediated phosphorylation of Spo7 was not majorly affected by the prephosphorylation with PKC. In the next set of experiments, the Nem1–Spo7 complex was prephosphorylated by PKA with unlabeled ATP and then phosphorylated by PKC with ^{32}P-labeled ATP (Fig. 9*B*). PKA caused a dose-dependent reduction (86%) of the subsequent phosphorylation of Spo7 by PKC, but the prephosphorylation of the complex by PKA had little effect on the subsequent phosphorylation of Nem1 by PKC.

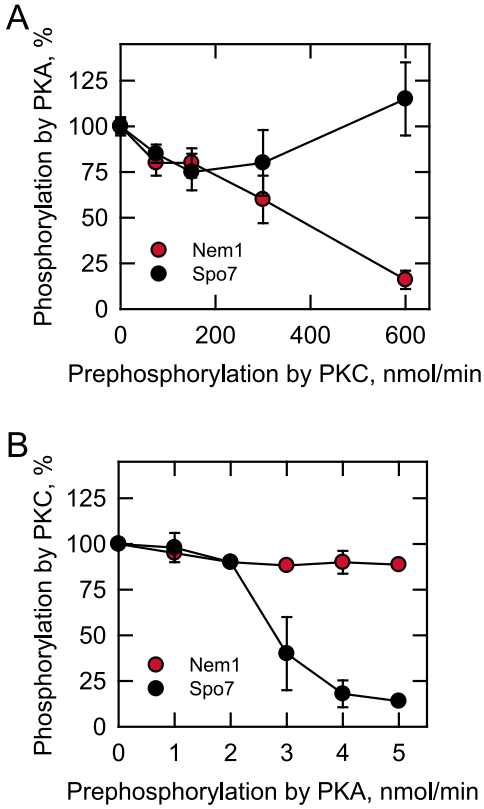

Figure 9. Prephosphorylation of the Nem1–Spo7 complex by PKC reduces the subsequent phosphorylation of Nem1 by PKA, and prephosphorylation of the complex by PKA reduces the subsequent phosphorylation of Spo7 by PKC. *A*, the purified Nem1–Spo7 complex was prephosphorylated by the indicated amounts of PKC for 60 min with unlabeled ATP (40 μM). The prephosphorylated complex was then phosphorylated by 8 units of PKA with 40 μM [γ-^{32}P]ATP for 20 min. *B*, the purified Nem1–Spo7 complex was prephosphorylated by the indicated amounts of PKA for 60 min with unlabeled ATP (40 μM). The prephosphorylated complex was then phosphorylated by 500 units of PKC with 40 μM [γ-^{32}P]ATP for 20 min. The ^{32}P-labeled Nem1 and Spo7 were separated from each other and the labeled ATP by SDS-PAGE and subjected to phosphorimaging and ImageQuant analyses. The amount of the phosphorylated Nem1 (*A*) or Spo7 (*B*) that was not subjected to prephosphorylation was set at 100%. The amount of PKC used in the experiment was greater than that of PKA because the PKA preparation is more active. Also, the units of the PKA and PKC activities are based on different peptide substrates. The data reported are the result of three independent experiments ±S.D. (*error bars*).

Discussion

Siniossoglou *et al.* (34) originally identified Nem1 and Spo7 as proteins that form a phosphatase complex in the nuclear/ER membrane and participate in nuclear envelope morphogenesis. Subsequently, Santos-Rosa *et al.* (11) have shown that the complex is a protein phosphatase, which dephosphorylates Pah1 for its role in nuclear membrane growth as well as in the transcriptional control of phospholipid synthesis gene expression. The Pah1 function is a key regulation point of PA utilization and lipid metabolism, which in turn has an impact on many aspects of cell physiology (7). Although much is known about the mode of action and the phosphorylation/dephosphorylation-mediated regulation of Pah1 (3–7), our understanding of the Nem1–Spo7 phosphatase regulation is limited. We know that the protein phosphatase has the pH optimum of 5.0 (29, 54). This is the approximate intracellular pH of yeast cells in the stationary phase (29, 54) when PA phosphatase activity and TAG levels are maximal and the bifurcation of PA toward lipid storage is favored over the synthesis of membrane phospholipids (12, 54, 55). Pah1 is phosphorylated on at least 40 sites (23, 37, 56–65), but not all of the protein kinases that phosphorylate the sites have been identified (7). Of the known protein kinase–target site relationships (24–28), the specificity of the Nem1–Spo7 phosphatase-mediated dephosphorylations is in the order of the sites phosphorylated by Pho85-Pho80 > PKA = casein kinase II > Cdc28-cyclin B > PKC (28, 29).

Although Nem1–Spo7 catalyzes the dephosphorylation of Pah1, the enzyme itself is subject to phosphorylation. Two of the protein kinases that are known to phosphorylate Pah1, namely PKA (26) and PKC (27), also phosphorylate Nem1 and Spo7 (39, 40). In a well-defined *in vitro* system, we demonstrated that Nem1 and Spo7 are phosphorylated by PKC. Both subunits were majorly phosphorylated on the serine residue with the threonine phosphorylation occurring to a minor extent. The enzymological studies performed with the purified

phosphatase complex confirmed that Nem1 and Spo7 are *bona fide* PKC substrates. Moreover, we showed that the PKC-mediated phosphorylation of the subunits occurs *in vivo*; endogenously phosphorylated Nem1 and Spo7 were recognized by the anti-phosphoserine PKC substrate antibody. Our biochemical and mutagenic studies with synthetic Nem1 and Spo7 peptides as well as the full-length Nem1 and Spo7 proteins led to the identification of Ser-201 in Nem1 and Ser-22/Ser-28 in Spo7 as the major sites of phosphorylation by PKC *in vitro*. *In vivo*, the phosphorylation-deficient alanine mutations of Ser-201 in Nem1 and Ser-22 and Ser-28 in Spo7 reduced the PKC-mediated phosphorylation of the subunits by 96 and 80%, respectively.

The phosphorylation of the WT complex had a small stimulatory effect on the Nem1–Spo7 phosphatase activity. We considered that this weak effect was influenced by the endogenous phosphorylations of the subunits. However, the phosphorylation of the alkaline phosphatase–treated complex by PKC did not have a significant effect on the phosphatase activity. Perhaps the phosphorylation of another site, as mediated by a different kinase, is required for the stimulation by PKC. However, the S201A mutation in Nem1 caused a 2-fold decrease in the Nem1–Spo7 phosphatase activity. This result supported the notion that the PKC-mediated phosphorylation of Nem1 stimulates the dephosphorylation of Pah1 by the complex. The phosphorylation of Spo7 by PKC does not appear to affect the Nem1–Spo7 phosphatase activity *per se*.

The temperature-sensitive phenotype imparted by the *nem1*Δ or *spo7*Δ mutation (34), like that caused by the *pah1*Δ mutation (1, 11, 19), is attributed to the defect in the synthesis of TAG (4, 7). The lipid analysis of the cells expressing the phosphorylation-deficient mutant forms of Nem1 and Spo7 indicated that PKC does not majorly affect TAG synthesis through the phosphorylations of Nem1 or Spo7. Thus, it is not too surprising that the phosphorylation-deficient mutations of Nem1 and Spo7 did not elicit the temperature-sensitive phenotype characteristic of cells with the *nem1*Δ and *spo7*Δ mutations. That the cells expressing these phosphorylation-deficient mutant forms of Nem1 or Spo7 grew at the restrictive temperature and had near normal levels of TAG indicated that the mutations did not affect their expression and the formation of the Nem1–Spo7 complex. This assertion is substantiated by the fact that the phosphorylation-deficient Nem1 and Spo7 were expressed and purified as a complex.

Although the lipid compositions of the cells expressing the phosphorylation-deficient Nem1 or Spo7 were not majorly different from that of the control cells, there were statistically significant effects imparted by the mutations. The most noticeable differences were in the exponential-phase cells where the S201A mutation in Nem1 or the S22A/S28A mutations in Spo7 caused a near 30% decrease in TAG content. This is consistent with a reduction in the Nem1-Spo7 phosphatase activity due to the S201A mutation in Nem1. Taken together, the data imply that PKC has a positive impact on TAG synthesis through the phosphorylation of the Nem1-Spo7 phosphatase.

PKA also phosphorylates the Nem1–Spo7 complex (40), but the consequence differs from that imposed by the PKC-mediated phosphorylation. PKA, which phosphorylates Nem1 at Ser-140 and Ser-210 and Spo7 at Ser-28 (Fig. 1*B*), has a negative impact on the *in vitro* activity of Nem1–Spo7 and on TAG synthesis (40). Interestingly, *in vitro*, the prephosphorylation of the complex by PKC had an inhibitory effect on the phosphorylation of Nem1 by PKA, and the prephosphorylation by PKA had an inhibitory effect on the phosphorylation of Spo7 by PKC. Thus, for Nem1, the phosphorylation of Ser-201 prevents phosphorylation at Ser-140 and/or Ser-210, but the opposite scenario of hierarchical phosphorylations does not apply. For Spo7, the inhibition of its PKC-mediated phosphorylation by PKA might be explained by the fact that Ser-28 is a phosphorylation site common to both kinases, and/or the phosphorylation of Ser-28 by PKA prevents the phosphorylation at Ser-22 by PKC. How these *in vitro* observations translate into the hierarchical phosphorylation that presumably occurs *in vivo* is not yet clear, but the fact that PKA and PKC have opposite effects on Nem1–Spo7 function may provide an explanation why the phosphorylation-site mutations of either PKC or PKA (40) do not have large effects on TAG content. This points to a fine-tuning mechanism that has been developed by nature to balance PA utilization and lipid metabolism.

Studies on the phosphorylation-mediated regulation of the yeast Nem1–Spo7 complex as well as of Pah1 are relevant to the regulation of PA utilization and lipid metabolism in higher eukaryotes, including humans (66–71). The mouse and human counterparts to Pah1 are lipins 1, 2, and 3 (72, 73), whereas the Nem1 and Spo7 counterparts are C-terminal domain nuclear envelope phosphatase 1 (CTDNEP1) (68) and nuclear envelope phosphatase 1–regulatory subunit 1 (NEP1-R1) (70), respectively. Lipin PA phosphatase enzymes are subject to phosphorylation, and the phosphorylated forms are dephosphorylated by the CTDNEP1–NEP1-R1 protein phosphatase complex (70, 74–77). High-throughput phosphoproteomics analyses (summarized on PhosphoSitePlus, www.phosphosite.org[4] (99)) indicate that both CTDNEP1 and NEP1-R1 are subject to phosphorylation. Analysis of the phosphorylation sites with the NetPhos3.1 algorithm (50) points to the possibility that they might be the targets of PKC. This information, coupled with the findings reported herein, provides the incentive to pursue this avenue of investigation with higher eukaryotic systems.

Experimental procedures

Materials and methods

Growth media were from Difco Laboratories. Avanti Polar Lipids was the source of all lipids. Enzyme reagents for DNA manipulations, carrier DNA for yeast transformation, and the QuikChange site-directed mutagenesis kit were obtained from New England Biolabs, Clontech, and Stratagene, respectively. Bio-Rad supplied the DNA size ladders, molecular mass protein standards, and reagents for electrophoresis, immunoblotting, and protein determination. SYPRO Ruby protein gel stain was from Invitrogen. Qiagen was the source of nickel-nitrilotriacetic acid-agarose resin and the plasmid DNA purification kits. MilliporeSigma was the supplier of ampicillin, kanamycin, chloramphenicol, BSA, 2-mercaptoethanol, isopropyl β-D-1-

[4] Please note that the JBC is not responsible for the long-term archiving and maintenance of this site or any other third party hosted site.

Table 1
Strains and plasmids used in this work

Strain or plasmid	Genotype or relevant characteristics	Source or Ref.
Strain		
E. coli		
DH5α	F^- ϕ80d*lacZ*ΔM15Δ (*lacZYA-argF*)U169 *deoR recA*1 *endA*1 *hsd*R17 (r_k^- m_k^+) *pho*A *sup*E44 λ^-*thi*-1 *gyr*A96 *rel*A1	78
BL21(DE3)pLysS	F^- *ompT hsdS*$_B$ ($r_B^-m_B^-$) *gal dcm* (DE3) pLysS	Novagen
BL21(DE3)	F^- *ompT hsdS*$_B$ ($r_B^-m_B^-$) *gal dcm* (DE3)	Invitrogen
S. cerevisiae		
BY4741	*MAT***a** *his3Δ1 leu2Δ0 met15Δ0 ura3Δ0*	Invitrogen
RS453	*MAT***a** *ade2–1 his3–11,15 leu2–3,112 trp1–1 ura3–52*	20
Derivatives		
SS1010	*nem1Δ::HIS3 spo7Δ::HIS3*	34
WMY161	*nem1Δ::URA3*	40
GHY67	*spo7Δ::URA3*	40
Plasmid		
pGH313	*PAH1* coding sequence inserted into pET-15b for *E. coli* expression	1
EB1164	*PHO85*-His$_6$ derivative of pQE-60 for *E. coli* expression	84
EB1076	*PHO80* derivative of pSBETA for *E. coli* expression	84
YCplac111-*GAL1/10-NEM1-PtA*	*NEM1-PtA* under control of *GAL1/10* promoter in *CEN/LEU2* vector	11
Derivative		
pPD115	*NEM1* (S201A)-*PtA*	This study
pRS314-*GAL1/10-SPO7*	*SPO7* under control of *GAL1/10* promoter in *CEN/TRP1* vector	40
Derivatives		
pPD121	*SPO7* (S22A) derivative of pRS314-*GAL1/10-SPO7*	This study
pWM211	*SPO7* (S28A) derivative of pRS314-*GAL1/10-SPO7*	40
pPD123	*SPO7* (S22A/S28A) derivative of pRS314-*GAL1/10-SPO7*	This study
pRS415	Low-copy *E. coli*/yeast shuttle vector with *LEU2*	94
Derivatives		
pPD221	*NEM1* inserted into pRS415	This study
pPD221(S201A)	*NEM1* (S201A)	This study
pGH443	*SPO7* inserted into pRS415	40
pGH443(S22A)	*SPO7* (S22A)	This study
pGH443(S28A)	*SPO7* (S28A)	40
pGH443(S22A/S28A)	*SPO7* (S22A/S28A)	This study

thiogalactoside, L-1-tosylamido-2-phenylethyl chloromethyl ketone–treated trypsin, PCR primers, nucleotides, Ponceau S stain, Triton X-100, protease inhibitors (phenylmethylsulfonyl fluoride, benzamidine, aprotinin, leupeptin, and pepstatin), phosphoamino acid standards, alkaline phosphatase–agarose, rabbit anti-protein A antibodies (product P3775, lot 025K4777), and TLC plates (cellulose and silica gel 60). GE Healthcare was the source of IgG-Sepharose, Sepharose, Q-Sepharose, PVDF membranes, and the enhanced chemifluorescence Western blotting detection kit. DE53 anion-exchange resin was purchased from Whatman. Promega was the source of bovine heart PKA catalytic subunit. Nem1 and Spo7 peptides used for PKC phosphorylation assays were synthesized by EZBioLabs. Rabbit anti-phosphoserine PKC substrate antibody (product 2261S, lot 23) was from Cell Signaling Technology. Thermo Scientific was the source of alkaline phosphatase–conjugated goat anti-rabbit IgG antibody (product 31340, lot NJ178812). P81 phosphocellulose paper was from Whatman. Radiochemicals were from PerkinElmer Life Sciences and scintillation-counting supplies were from National Diagnostics. All other chemicals were reagent-grade.

Strains, plasmids, and growth conditions

Table 1 contains a list of the *E. coli* and *S. cerevisiae* strains and the plasmids used in this study. The isolation of chromosomal and plasmid DNA, the digestion and ligation of DNA, and PCR were performed according to standard protocols (78). *E. coli* (78) and *S. cerevisiae* (79) transformations were performed as described previously. A 2.8-kb DNA fragment containing the *NEM1* gene was amplified by PCR (80) from strain BY4741. The *NEM1* gene was inserted (XhoI/NotI sites) into plasmid pRS415 to produce plasmid pPD221. The S201A mutation of *NEM1* and the S22A, S28A, and S22A/S28A mutations of *SPO7* were made by PCR-mediated site-directed mutagenesis using the appropriate PCR primers and templates as described by Choi *et al.* (24) to produce the plasmids listed in Table 1. DNA sequencing of the PCR products was used to confirm the mutations of the *NEM1* and *SPO7* coding sequences. For the expression and purification of WT and phosphorylation-deficient mutant proteins, the YCplac111-*GAL1/10-NEM1-PtA* and pRS313-*GAL1/10-SPO7* plasmids and their derivatives were transformed into the *S. cerevisiae* mutant *nem1Δ::HIS3 spo7Δ::HIS* (SS1010). To analyze the effects of the phosphorylation-deficient mutations on growth and lipid composition, the plasmids pPD221 (*NEM1*) or pGH443 (*SPO7*) and their derivatives were transformed into the yeast mutants *nem1Δ::URA3* (WMY161) and *spo7Δ::URA3* (GHY67), respectively.

All plasmids were propagated in the *E. coli* strain DH5α, whereas the *E. coli* strains BL21(DE3)pLysS and BL21(DE3) were used to express His$_6$-tagged Pah1 and His$_6$-tagged Pho85 and Pho80, respectively. The *E. coli* cells were grown at 37 °C in lysogeny broth medium (1% tryptone, 0.5% yeast extract, 1% NaCl (pH 7.0)). For the selection of the transformant cells carrying plasmids, the growth medium was supplemented with antibiotics (*e.g.* 100 μg/ml ampicillin, 30 μg/ml kanamycin, and 34 μg/ml chloramphenicol). The expressions of His$_6$-tagged Pah1, His$_6$-tagged Pho85, and Pho80 were induced with 1 mM isopropyl β-D-thiogalactoside. The *S. cerevisiae* cells were routinely grown at 30 °C in synthetic complete medium (81) containing 2% glucose; appropriate amino acids were omitted from the growth medium to select for cells carrying specific plasmids. For the galactose-induced expressions of protein

A-tagged Nem1 and Spo7, the yeast cells were first grown to the exponential phase in synthetic complete medium with 2% raffinose and then grown in the same medium for 8 h with 2% galactose. For the growth spot test, cells were grown on synthetic complete medium agar plates (81). Cell numbers in liquid cultures were determined spectrophotometrically at 600 nm. Solid medium plates were prepared by dissolving agar (1.5% for *E. coli* and 2% for *S. cerevisiae*) into the lipid growth medium.

Purification of enzymes and protein determinations

PKC fused with a ZZ tag (two repeats of the 60-amino-acid IgG-binding domain of *Staphylococcus aureus* protein A) was expressed in yeast (confirmed by immunoblotting with anti-protein A antibody) and purified by chromatography with DE53 and IgG-Sepharose as described by Antonsson *et al.* (82) with minor modifications (43). The purified enzyme was dialyzed against 50 mM Tris-HCl (pH 7.5) buffer containing 15% glycerol. The WT and mutant forms of the Nem1–Spo7 complex (Nem1 tagged with protein A) were purified from the yeast cells by IgG-Sepharose affinity chromatography as described by Siniossoglou *et al.* (83) with minor modifications (29). His_6-tagged Pah1 expressed in *E. coli* was purified by affinity chromatography with nickel-nitrilotriacetic acid-agarose (1) followed by Q-Sepharose chromatography as described by Su *et al.* (29). The *E. coli*– expressed His_6-tagged Pho85–Pho80 protein kinase complex was purified by nickel-nitrilotriacetic acid-agarose affinity chromatography (84). SDS-PAGE (85) analysis indicated that the enzyme preparations were highly pure. The protein concentration was estimated by the method of Bradford (86) or by ImageQuant analysis of Coomassie Blue–stained or SYPRO Ruby–stained SDS-polyacrylamide gels. BSA was used as a standard to estimate protein concentrations in solution or in polyacrylamide gels.

SDS-PAGE and immunoblotting

SDS-PAGE (85) was routinely performed with a 12% slab gel, and immunoblotting (87, 88) was performed with a PVDF membrane. Equal amounts of protein were loaded onto the SDS-polyacrylamide gels, and Ponceau S staining was used to monitor the protein transfer from the polyacrylamide gel to the PVDF membrane. The affinity-purified IgG fractions of rabbit anti-Nem1 and anti-Spo7 antibodies (40) were used at a protein concentration of 1 μg/ml. The rabbit anti-protein A and anti-phosphoserine PKC substrate antibodies were used at dilutions of 1:3,000 and 1:1,000, respectively. Alkaline phosphatase–conjugated goat anti-rabbit IgG antibody was used at a dilution of 1:5,000. Immune complexes were detected using the enhanced chemifluorescence immunoblotting substrate. Fluorimaging was used to acquire fluorescence signals from immunoblots, and the intensities of the images were analyzed by ImageQuant software. A standard curve was used to determine that the immunoblot signals were in the linear range of detection.

Phosphorylation reactions

Phosphorylation reactions were performed in triplicate for 20 min at 30 °C in a total volume of 20 μl. The standard reaction mixture for PKC contained 50 mM Tris-HCl (pH 7.5), 10 mM $MgCl_2$, 10 mM 2-mercaptoethanol, 1.7 mM $CaCl_2$, 500 μM PS, 150 μM DAG, 50 μM [γ-^{32}P]ATP (3,000 cpm/pmol), and the indicated amounts of the Nem1–Spo7 complex and PKC (39). PS, DAG, and $CaCl_2$ were omitted from the PKC reaction mixture when the Nem1 and Spo7 peptides were used as substrates (39). The PKC reactions with the Nem1–Spo7 complex were terminated by mixing with Laemmli buffer (85), resolved by SDS-PAGE, and transferred to a PVDF membrane for phosphorimaging analysis. Alternatively, the SDS-polyacrylamide gel was dried and subjected to the analysis, and the radioactive signal was quantified with ImageQuant software. In the PKC assays with Nem1 or Spo7 peptides, the enzyme reaction was terminated by spotting the reaction mixture onto a P81 phosphocellulose paper. The paper was washed three times with 75 mM phosphoric acid and then subjected to scintillation counting. A unit of PKC activity was defined as 1 nmol/min. The phosphorylation by PKA was measured similarly; the reaction mixture contained 25 mM Tris-HCl (pH 7.5), 10 mM $MgCl_2$, 2 mM DTT, 100 μM [γ-^{32}P]ATP (3,000 cpm/pmol), and the indicated amounts of the Nem1–Spo7 complex and PKA (40). A unit of PKA activity was defined as 1 nmol/min.

Phosphoamino acid analysis and phosphopeptide mapping

PVDF membrane slices containing radioactively labeled Nem1 or Spo7 were subjected to hydrolysis with 6 N HCl at 110 °C (for phosphoamino acid analysis) or proteolytic digestion with L-1-tosylamido-2-phenylethyl chloromethyl ketone–treated trypsin (for phosphopeptide mapping) as described previously (42, 89, 90). The acid hydrolysates were mixed with standard phosphoamino acids and separated by two-dimensional electrophoresis on cellulose TLC plates (89). Phosphoamino acid standards were visualized by ninhydrin staining, whereas the ^{32}P-labeled phosphoamino acids were observed by phosphorimaging analysis. The tryptic digests were separated on the cellulose plates first by electrophoresis and then by TLC (89). The radioactive phosphopeptides were visualized by phosphorimaging analysis.

Nem1–Spo7 enzyme assay

The phosphatase activity of Nem1–Spo7 was measured for 10 min at 30 °C by following the release of $^{32}P_i$ from [^{32}P]Pah1, which was prepared by the Pho85–Pho80 phosphorylation of *E. coli*– expressed Pah1 (29). The reaction mixture contained 100 mM sodium acetate (pH 5.0), 10 mM $MgCl_2$, 0.25 mM Triton X-100, 1 mM DTT, 0.25 μM phosphorylated Pah1, and the Nem1–Spo7 complex in a total volume of 50 μl. The amount of phosphate produced in the reaction was calculated on the basis of the specific activity of the [γ-^{32}P]ATP used to prepare [^{32}P]Pah1 (29). A unit of Nem1–Spo7 phosphatase activity was defined as the amount of enzyme that catalyzed the formation of 1 nmol of phosphate/min.

Radiolabeling and lipid analysis

The steady-state labeling of lipids with [2-^{14}C]acetate (91), the extraction of lipids from the radiolabeled cells (92), and their separation by one-dimensional TLC (93) were performed as described previously. The resolved lipids were observed by

phosphorimaging and quantified by ImageQuant software. The identity of radiolabeled lipids was confirmed by comparison with the migration of authentic standards visualized by staining with iodine vapor.

Data analysis

Excel software was used for statistical analyses where p values <0.05 were taken as a significant difference. The Enzyme Kinetics module of SigmaPlot software, which uses the Marquardt–Levenberg algorithm, was used to determine kinetic parameters according to the Michaelis–Menten equation.

Author contributions—P. D., W.-M. S., M. M., G.-S. H., and G. M. C. conceptualization; P. D., W.-M. S., G.-S. H., and G. M. C. data curation; P. D., W.-M. S., M. M., G.-S. H., and G. M. C. formal analysis; P. D., W.-M. S., G.-S. H., and G. M. C. validation; P. D., W.-M. S., M. M., G.-S. H., and G. M. C. investigation; P. D., W.-M. S., M. M., G.-S. H., and G. M. C. visualization; P. D., W.-M. S., M. M., G.-S. H., and G. M. C. methodology; P. D. writing-original draft; W.-M. S., M. M., G.-S. H., and G. M. C. writing-review and editing; G. M. C. supervision; G. M. C. funding acquisition; G. M. C. project administration.

Acknowledgments—We thank Azam Hassaninasab and Yeonhee Park for helpful discussions during this work.

References

1. Han, G.-S., Wu, W.-I., and Carman, G. M. (2006) The *Saccharomyces cerevisiae* lipin homolog is a Mg^{2+}-dependent phosphatidate phosphatase enzyme. *J. Biol. Chem.* **281,** 9210–9218 CrossRef Medline
2. Smith, S. W., Weiss, S. B., and Kennedy, E. P. (1957) The enzymatic dephosphorylation of phosphatidic acids. *J. Biol. Chem.* **228,** 915–922 Medline
3. Carman, G. M., and Han, G.-S. (2009) Phosphatidic acid phosphatase, a key enzyme in the regulation of lipid synthesis. *J. Biol. Chem.* **284,** 2593–2597 CrossRef Medline
4. Pascual, F., and Carman, G. M. (2013) Phosphatidate phosphatase, a key regulator of lipid homeostasis. *Biochim. Biophys. Acta* **1831,** 514–522 CrossRef Medline
5. Carman, G. M., and Han, G. S. (2019) Fat-regulating phosphatidic acid phosphatase: a review of its roles and regulation in lipid homeostasis. *J. Lipid Res.* **60,** 2–6 CrossRef Medline
6. Carman, G. M. (2019) Discoveries of the phosphatidate phosphatase genes in yeast published in the *Journal of Biological Chemistry*. *J. Biol. Chem.* **294,** 1681–1689 CrossRef Medline
7. Kwiatek, J. M., Han, G. S., and Carman, G. M. (2019) Phosphatidate-mediated regulation of lipid synthesis at the nuclear/endoplasmic reticulum membrane. *Biochim. Biophys. Acta Mol. Cell Biol. Lipids*, in press CrossRef Medline
8. Adeyo, O., Horn, P. J., Lee, S., Binns, D. D., Chandrahas, A., Chapman, K. D., and Goodman, J. M. (2011) The yeast lipin orthologue Pah1p is important for biogenesis of lipid droplets. *J. Cell Biol.* **192,** 1043–1055 CrossRef Medline
9. Fakas, S., Qiu, Y., Dixon, J. L., Han, G.-S., Ruggles, K. V., Garbarino, J., Sturley, S. L., and Carman, G. M. (2011) Phosphatidate phosphatase activity plays a key role in protection against fatty acid-induced toxicity in yeast. *J. Biol. Chem.* **286,** 29074–29085 CrossRef Medline
10. Hassaninasab, A., Han, G.-S., and Carman, G. M. (2017) Tips on the analysis of phosphatidic acid by the fluorometric coupled enzyme assay. *Anal. Biochem.* **526,** 69–70 CrossRef Medline
11. Santos-Rosa, H., Leung, J., Grimsey, N., Peak-Chew, S., and Siniossoglou, S. (2005) The yeast lipin Smp2 couples phospholipid biosynthesis to nuclear membrane growth. *EMBO J.* **24,** 1931–1941 CrossRef Medline
12. Pascual, F., Soto-Cardalda, A., and Carman, G. M. (2013) *PAH1*-encoded phosphatidate phosphatase plays a role in the growth phase- and inositol-mediated regulation of lipid synthesis in *Saccharomyces cerevisiae*. *J. Biol. Chem.* **288,** 35781–35792 CrossRef Medline
13. Han, G.-S., and Carman, G. M. (2017) Yeast *PAH1*-encoded phosphatidate phosphatase controls the expression of *CHO1*-encoded phosphatidylserine synthase for membrane phospholipid synthesis. *J. Biol. Chem.* **292,** 13230–13242 CrossRef Medline
14. Sasser, T., Qiu, Q. S., Karunakaran, S., Padolina, M., Reyes, A., Flood, B., Smith, S., Gonzales, C., and Fratti, R. A. (2012) The yeast lipin 1 orthologue Pah1p regulates vacuole homeostasis and membrane fusion. *J. Biol. Chem.* **287,** 2221–2236 CrossRef Medline
15. Lussier, M., White, A. M., Sheraton, J., di Paolo, T., Treadwell, J., Southard, S. B., Horenstein, C. I., Chen-Weiner, J., Ram, A. F., Kapteyn, J. C., Roemer, T. W., Vo, D. H., Bondoc, D. C., Hall, J., Zhong, W. W., *et al.* (1997) Large scale identification of genes involved in cell surface biosynthesis and architecture in *Saccharomyces cerevisiae*. *Genetics* **147,** 435–450 Medline
16. Ruiz, C., Cid, V. J., Lussier, M., Molina, M., and Nombela, C. (1999) A large-scale sonication assay for cell wall mutant analysis in yeast. *Yeast* **15,** 1001–1008 CrossRef Medline
17. Park, Y., Han, G. S., Mileykovskaya, E., Garrett, T. A., and Carman, G. M. (2015) Altered lipid synthesis by lack of yeast Pah1 phosphatidate phosphatase reduces chronological life span. *J. Biol. Chem.* **290,** 25382–25394 CrossRef Medline
18. Han, G.-S., Siniossoglou, S., and Carman, G. M. (2007) The cellular functions of the yeast lipin homolog Pah1p are dependent on its phosphatidate phosphatase activity. *J. Biol. Chem.* **282,** 37026–37035 CrossRef Medline
19. Irie, K., Takase, M., Araki, H., and Oshima, Y. (1993) A gene, SMP2, involved in plasmid maintenance and respiration in *Saccharomyces cerevisiae* encodes a highly charged protein. *Mol. Gen. Genet.* **236,** 283–288 Medline
20. Han, G.-S., O'Hara, L., Carman, G. M., and Siniossoglou, S. (2008) An unconventional diacylglycerol kinase that regulates phospholipid synthesis and nuclear membrane growth. *J. Biol. Chem.* **283,** 20433–20442 CrossRef Medline
21. Córcoles-Sáez, I., Hernández, M. L., Martínez-Rivas, J. M., Prieto, J. A., and Randez-Gil, F. (2016) Characterization of the *S. cerevisiae* inp51 mutant links phosphatidylinositol 4,5-bisphosphate levels with lipid content, membrane fluidity and cold growth. *Biochim. Biophys. Acta* **1861,** 213–226 CrossRef Medline
22. Rahman, M. A., Mostofa, M. G., and Ushimaru, T. (2018) The Nem1/Spo7-Pah1/lipin axis is required for autophagy induction after TORC1 inactivation. *FEBS J.* **285,** 1840–1860 CrossRef Medline
23. O'Hara, L., Han, G.-S., Peak-Chew, S., Grimsey, N., Carman, G. M., and Siniossoglou, S. (2006) Control of phospholipid synthesis by phosphorylation of the yeast lipin Pah1p/Smp2p Mg^{2+}-dependent phosphatidate phosphatase. *J. Biol. Chem.* **281,** 34537–34548 CrossRef Medline
24. Choi, H.-S., Su, W.-M., Morgan, J. M., Han, G.-S., Xu, Z., Karanasios, E., Siniossoglou, S., and Carman, G. M. (2011) Phosphorylation of phosphatidate phosphatase regulates its membrane association and physiological functions in *Saccharomyces cerevisiae:* identification of Ser^{602}, Thr^{723}, and Ser^{744} as the sites phosphorylated by *CDC28* (*CDK1*)-encoded cyclin-dependent kinase. *J. Biol. Chem.* **286,** 1486–1498 CrossRef Medline
25. Choi, H.-S., Su, W.-M., Han, G.-S., Plote, D., Xu, Z., and Carman, G. M. (2012) Pho85p-Pho80p phosphorylation of yeast Pah1p phosphatidate phosphatase regulates its activity, location, abundance, and function in lipid metabolism. *J. Biol. Chem.* **287,** 11290–11301 CrossRef Medline
26. Su, W.-M., Han, G.-S., Casciano, J., and Carman, G. M. (2012) Protein kinase A-mediated phosphorylation of Pah1p phosphatidate phosphatase functions in conjunction with the Pho85p-Pho80p and Cdc28p-cyclin B kinases to regulate lipid synthesis in yeast. *J. Biol. Chem.* **287,** 33364–33376 CrossRef Medline
27. Su, W.-M., Han, G.-S., and Carman, G. M. (2014) Cross-talk phosphorylations by protein kinase C and Pho85p-Pho80p protein kinase regulate Pah1p phosphatidate phosphatase abundance in *Saccharomyces cerevisiae*. *J. Biol. Chem.* **289,** 18818–18830 CrossRef Medline
28. Hsieh, L.-S., Su, W.-M., Han, G.-S., and Carman, G. M. (2016) Phosphorylation of yeast Pah1 phosphatidate phosphatase by casein kinase II regulates its function in lipid metabolism. *J. Biol. Chem.* **291,** 9974–9990 CrossRef Medline

29. Su, W.-M., Han, G.-S., and Carman, G. M. (2014) Yeast Nem1-Spo7 protein phosphatase activity on Pah1 phosphatidate phosphatase is specific for the Pho85-Pho80 protein kinase phosphorylation sites. *J. Biol. Chem.* **289,** 34699–34708 CrossRef Medline
30. Karanasios, E., Han, G.-S., Xu, Z., Carman, G. M., and Siniossoglou, S. (2010) A phosphorylation-regulated amphipathic helix controls the membrane translocation and function of the yeast phosphatidate phosphatase. *Proc. Natl. Acad. Sci. U.S.A.* **107,** 17539–17544 CrossRef Medline
31. Karanasios, E., Barbosa, A. D., Sembongi, H., Mari, M., Han, G.-S., Reggiori, F., Carman, G. M., and Siniossoglou, S. (2013) Regulation of lipid droplet and membrane biogenesis by the acidic tail of the phosphatidate phosphatase Pah1p. *Mol. Biol. Cell* **24,** 2124–2133 CrossRef Medline
32. Pascual, F., Hsieh, L.-S., Soto-Cardalda, A., and Carman, G. M. (2014) Yeast Pah1p phosphatidate phosphatase is regulated by proteasome-mediated degradation. *J. Biol. Chem.* **289,** 9811–9822 CrossRef Medline
33. Hsieh, L.-S., Su, W.-M., Han, G.-S., and Carman, G. M. (2015) Phosphorylation regulates the ubiquitin-independent degradation of yeast Pah1 phosphatidate phosphatase by the 20S proteasome. *J. Biol. Chem.* **290,** 11467–11478 CrossRef Medline
34. Siniossoglou, S., Santos-Rosa, H., Rappsilber, J., Mann, M., and Hurt, E. (1998) A novel complex of membrane proteins required for formation of a spherical nucleus. *EMBO J.* **17,** 6449–6464 CrossRef Medline
35. Xu, X., and Okamoto, K. (2018) The Nem1-Spo7 protein phosphatase complex is required for efficient mitophagy in yeast. *Biochem. Biophys. Res. Commun.* **496,** 51–57 CrossRef Medline
36. Holt, L. J., Tuch, B. B., Villén, J., Johnson, A. D., Gygi, S. P., and Morgan, D. O. (2009) Global analysis of Cdk1 substrate phosphorylation sites provides insights into evolution. *Science* **325,** 1682–1686 CrossRef Medline
37. Swaney, D. L., Beltrao, P., Starita, L., Guo, A., Rush, J., Fields, S., Krogan, N. J., and Villén, J. (2013) Global analysis of phosphorylation and ubiquitylation cross-talk in protein degradation. *Nat. Methods* **10,** 676–682 CrossRef Medline
38. Dubots, E., Cottier, S., Péli-Gulli, M. P., Jaquenoud, M., Bontron, S., Schneiter, R., and De Virgilio, C. (2014) TORC1 regulates Pah1 phosphatidate phosphatase activity via the Nem1/Spo7 protein phosphatase complex. *PLoS One* **9,** e104194 CrossRef Medline
39. Dey, P., Su, W. M., Han, G. S., and Carman, G. M. (2017) Phosphorylation of lipid metabolic enzymes by yeast Pkc1 protein kinase C requires phosphatidylserine and diacylglycerol. *J. Lipid Res.* **58,** 742–751 CrossRef Medline
40. Su, W.-M., Han, G. S., Dey, P., and Carman, G. M. (2018) Protein kinase A phosphorylates the Nem1-Spo7 protein phosphatase complex that regulates the phosphorylation state of the phosphatidate phosphatase Pah1 in yeast. *J. Biol. Chem.* **293,** 15801–15814 CrossRef Medline
41. Levin, D. E., Fields, F. O., Kunisawa, R., Bishop, J. M., and Thorner, J. (1990) A candidate protein kinase C gene, PKC1, is required for the *S. cerevisiae* cell cycle. *Cell* **62,** 213–224 CrossRef Medline
42. Yang, W.-L., and Carman, G. M. (1995) Phosphorylation of CTP synthetase from *Saccharomyces cerevisiae* by protein kinase C. *J. Biol. Chem.* **270,** 14983–14988 CrossRef Medline
43. Yang, W.-L., Bruno, M. E., and Carman, G. M. (1996) Regulation of yeast CTP synthetase activity by protein kinase C. *J. Biol. Chem.* **271,** 11113–11119 CrossRef Medline
44. Park, T.-S., O'Brien, D. J., and Carman, G. M. (2003) Phosphorylation of CTP synthetase on Ser^{36}, Ser^{330}, Ser^{354}, and Ser^{454} regulates the levels of CTP and phosphatidylcholine synthesis in *Saccharomyces cerevisiae*. *J. Biol. Chem.* **278,** 20785–20794 CrossRef Medline
45. Choi, M.-G., Park, T. S., and Carman, G. M. (2003) Phosphorylation of *Saccharomyces cerevisiae* CTP synthetase at Ser^{424} by protein kinases A and C regulates phosphatidylcholine synthesis by the CDP-choline pathway. *J. Biol. Chem.* **278,** 23610–23616 CrossRef Medline
46. Choi, M.-G., Kurnov, V., Kersting, M. C., Sreenivas, A., and Carman, G. M. (2005) Phosphorylation of the yeast choline kinase by protein kinase C. Identification of Ser^{25} and Ser^{30} as major sites of phosphorylation. *J. Biol. Chem.* **280,** 26105–26112 CrossRef Medline
47. Sreenivas, A., Villa-Garcia, M. J., Henry, S. A., and Carman, G. M. (2001) Phosphorylation of the yeast phospholipid synthesis regulatory protein Opi1p by protein kinase C. *J. Biol. Chem.* **276,** 29915–29923 CrossRef Medline
48. Levin, D. E., and Bartlett-Heubusch, E. (1992) Mutants in the *S. cerevisiae PKC1* gene display a cell cycle-specific osmotic stability defect. *J. Cell Biol.* **116,** 1221–1229 CrossRef Medline
49. Kamada, Y., Jung, U. S., Piotrowski, J., and Levin, D. E. (1995) The protein kinase C-activated MAP kinase pathway of *Saccharomyces cerevisiae* mediates a novel aspect of the heat shock response. *Genes Dev.* **9,** 1559–1571 CrossRef Medline
50. Blom, N., Sicheritz-Pontén, T., Gupta, R., Gammeltoft, S., and Brunak, S. (2004) Prediction of post-translational glycosylation and phosphorylation of proteins from the amino acid sequence. *Proteomics* **4,** 1633–1649 CrossRef Medline
51. Ingrell, C. R., Miller, M. L., Jensen, O. N., and Blom, N. (2007) NetPhosYeast: prediction of protein phosphorylation sites in yeast. *Bioinformatics* **23,** 895–897 CrossRef Medline
52. Brot, F. E., and Bender, M. L. (1969) Use of the specificity constant of α-chymotrypsin. *J. Am. Chem. Soc.* **91,** 7187–7191 CrossRef
53. Siniossoglou, S. (2013) Phospholipid metabolism and nuclear function: roles of the lipin family of phosphatidic acid phosphatases. *Biochim. Biophys. Acta* **1831,** 575–581 CrossRef Medline
54. Barbosa, A. D., Sembongi, H., Su, W.-M., Abreu, S., Reggiori, F., Carman, G. M., and Siniossoglou, S. (2015) Lipid partitioning at the nuclear envelope controls membrane biogenesis. *Mol. Biol. Cell* **26,** 3641–3657 CrossRef Medline
55. Orij, R., Urbanus, M. L., Vizeacoumar, F. J., Giaever, G., Boone, C., Nislow, C., Brul, S., and Smits, G. J. (2012) Genome-wide analysis of intracellular pH reveals quantitative control of cell division rate by pH_c in *Saccharomyces cerevisiae*. *Genome Biol.* **13,** R80 CrossRef Medline
56. Gruhler, A., Olsen, J. V., Mohammed, S., Mortensen, P., Faergeman, N. J., Mann, M., and Jensen, O. N. (2005) Quantitative phosphoproteomics applied to the yeast pheromone signaling pathway. *Mol. Cell. Proteomics* **4,** 310–327 CrossRef Medline
57. Li, X., Gerber, S. A., Rudner, A. D., Beausoleil, S. A., Haas, W., Villén, J., Elias, J. E., and Gygi, S. P. (2007) Large-scale phosphorylation analysis of α-factor-arrested *Saccharomyces cerevisiae*. *J. Proteome. Res.* **6,** 1190–1197 CrossRef Medline
58. Chi, A., Huttenhower, C., Geer, L. Y., Coon, J. J., Syka, J. E., Bai, D. L., Shabanowitz, J., Burke, D. J., Troyanskaya, O. G., and Hunt, D. F. (2007) Analysis of phosphorylation sites on proteins from *Saccharomyces cerevisiae* by electron transfer dissociation (ETD) mass spectrometry. *Proc. Natl. Acad. Sci. U.S.A.* **104,** 2193–2198 CrossRef Medline
59. Smolka, M. B., Albuquerque, C. P., Chen, S. H., and Zhou, H. (2007) Proteome-wide identification of *in vivo* targets of DNA damage checkpoint kinases. *Proc. Natl. Acad. Sci. U.S.A.* **104,** 10364–10369 CrossRef Medline
60. Albuquerque, C. P., Smolka, M. B., Payne, S. H., Bafna, V., Eng, J., and Zhou, H. (2008) A multidimensional chromatography technology for in-depth phosphoproteome analysis. *Mol. Cell. Proteomics* **7,** 1389–1396 CrossRef Medline
61. Soufi, B., Kelstrup, C. D., Stoehr, G., Fröhlich, F., Walther, T. C., and Olsen, J. V. (2009) Global analysis of the yeast osmotic stress response by quantitative proteomics. *Mol. Biosyst.* **5,** 1337–1346 CrossRef Medline
62. Gnad, F., de Godoy, L. M., Cox, J., Neuhauser, N., Ren, S., Olsen, J. V., and Mann, M. (2009) High-accuracy identification and bioinformatic analysis of *in vivo* protein phosphorylation sites in yeast. *Proteomics* **9,** 4642–4652 CrossRef Medline
63. Helbig, A. O., Rosati, S., Pijnappel, P. W., van Breukelen, B., Timmers, M. H., Mohammed, S., Slijper, M., and Heck, A. J. (2010) Perturbation of the yeast *N*-acetyltransferase NatB induces elevation of protein phosphorylation levels. *BMC Genomics* **11,** 685 CrossRef Medline
64. Soulard, A., Cremonesi, A., Moes, S., Schütz, F., Jenö, P., and Hall, M. N. (2010) The rapamycin-sensitive phosphoproteome reveals that TOR controls protein kinase A toward some but not all substrates. *Mol. Biol. Cell* **21,** 3475–3486 CrossRef Medline
65. Bodenmiller, B., Wanka, S., Kraft, C., Urban, J., Campbell, D., Pedrioli, P. G., Gerrits, B., Picotti, P., Lam, H., Vitek, O., Brusniak, M. Y., Roschitzki, B., Zhang, C., Shokat, K. M., Schlapbach, R., *et al.* (2010) Phosphopro-

teomic analysis reveals interconnected system-wide responses to perturbations of kinases and phosphatases in yeast. *Sci. Signal.* **3,** rs4 CrossRef Medline
66. Csaki, L. S., Dwyer, J. R., Fong, L. G., Tontonoz, P., Young, S. G., and Reue, K. (2013) Lipins, lipinopathies, and the modulation of cellular lipid storage and signaling. *Prog. Lipid Res.* **52,** 305–316 CrossRef Medline
67. Zhang, P., and Reue, K. (2017) Lipin proteins and glycerolipid metabolism: roles at the ER membrane and beyond. *Biochim. Biophys. Acta Biomembr.* **1859,** 1583–1595 CrossRef Medline
68. Kim, Y., Gentry, M. S., Harris, T. E., Wiley, S. E., Lawrence, J. C., Jr., and Dixon, J. E. (2007) A conserved phosphatase cascade that regulates nuclear membrane biogenesis. *Proc. Natl. Acad. Sci. U.S.A.* **104,** 6596–6601 CrossRef Medline
69. Wu, R., Garland, M., Dunaway-Mariano, D., and Allen, K. N. (2011) *Homo sapiens* Dullard protein phosphatase shows a preference for the insulin-dependent phosphorylation site of lipin1. *Biochemistry* **50,** 3045–3047 CrossRef Medline
70. Han, S., Bahmanyar, S., Zhang, P., Grishin, N., Oegema, K., Crooke, R., Graham, M., Reue, K., Dixon, J. E., and Goodman, J. M. (2012) Nuclear envelope phosphatase 1-regulatory subunit 1 (formerly TMEM188) is the metazoan Spo7p ortholog and functions in the lipin activation pathway. *J. Biol. Chem.* **287,** 3123–3137 CrossRef Medline
71. Reue, K., and Wang, H. (2019) Mammalian lipin phosphatidic acid phosphatases in lipid synthesis and beyond: metabolic and inflammatory disorders. *J. Lipid Res.* **60,** 728–733 CrossRef Medline
72. Péterfy, M., Phan, J., Xu, P., and Reue, K. (2001) Lipodystrophy in the *fld* mouse results from mutation of a new gene encoding a nuclear protein, lipin. *Nat. Genet.* **27,** 121–124 CrossRef Medline
73. Donkor, J., Sariahmetoglu, M., Dewald, J., Brindley, D. N., and Reue, K. (2007) Three mammalian lipins act as phosphatidate phosphatases with distinct tissue expression patterns. *J. Biol. Chem.* **282,** 3450–3457 CrossRef Medline
74. Harris, T. E., Huffman, T. A., Chi, A., Shabanowitz, J., Hunt, D. F., Kumar, A., and Lawrence, J. C., Jr. (2007) Insulin controls subcellular localization and multisite phosphorylation of the phosphatidic acid phosphatase, lipin 1. *J. Biol. Chem.* **282,** 277–286 CrossRef Medline
75. Chang, H. J., Jesch, S. A., Gaspar, M. L., and Henry, S. A. (2004) Role of the unfolded protein response pathway in secretory stress and regulation of *INO1* expression in *Saccharomyces cerevisiae*. *Genetics* **168,** 1899–1913 CrossRef Medline
76. Boroda, S., Takkellapati, S., Lawrence, R. T., Entwisle, S. W., Pearson, J. M., Granade, M. E., Mullins, G. R., Eaton, J. M., Villén, J., and Harris, T. E. (2017) The phosphatidic acid-binding, polybasic domain is responsible for the differences in the phosphoregulation of lipins 1 and 3. *J. Biol. Chem.* **292,** 20481–20493 CrossRef Medline
77. Eaton, J. M., Mullins, G. R., Brindley, D. N., and Harris, T. E. (2013) Phosphorylation of lipin 1 and charge on the phosphatidic acid head group control its phosphatidic acid phosphatase activity and membrane association. *J. Biol. Chem.* **288,** 9933–9945 CrossRef Medline
78. Sambrook, J., Fritsch, E. F., and Maniatis, T. (1989) *Molecular Cloning: A Laboratory Manual*, 2nd Ed., Cold Spring Harbor Laboratory, Cold Spring Harbor, NY
79. Ito, H., Fukuda, Y., Murata, K., and Kimura, A. (1983) Transformation of intact yeast cells treated with alkali cations. *J. Bacteriol.* **153,** 163–168 Medline
80. Saiki, R. K., Scharf, S., Faloona, F., Mullis, K. B., Horn, G. T., Erlich, H. A., and Arnheim, N. (1985) Enzymatic amplification of β-globin genomic sequences and restriction site analysis for diagnosis of sickle cell anemia. *Science* **230,** 1350–1354 CrossRef Medline
81. Rose, M. D., Winston, F., and Heiter, P. (1990) *Methods in Yeast Genetics: A Laboratory Course Manual*, Cold Spring Harbor Laboratory Press, Cold Spring Harbor, NY
82. Antonsson, B., Montessuit, S., Friedli, L., Payton, M. A., and Paravicini, G. (1994) Protein kinase C in yeast. Characteristics of the *Saccharomyces cerevisiae PKC1* gene product. *J. Biol. Chem.* **269,** 16821–16828 Medline
83. Siniossoglou, S., Hurt, E. C., and Pelham, H. R. (2000) Psr1p/Psr2p, two plasma membrane phosphatases with an essential D*X*D*X*(T/V) motif required for sodium stress response in yeast. *J. Biol. Chem.* **275,** 19352–19360 CrossRef Medline
84. Jeffery, D. A., Springer, M., King, D. S., and O'Shea, E. K. (2001) Multi-site phosphorylation of Pho4 by the cyclin-CDK Pho80-Pho85 is semi-processive with site preference. *J. Mol. Biol.* **306,** 997–1010 CrossRef Medline
85. Laemmli, U. K. (1970) Cleavage of structural proteins during the assembly of the head of bacteriophage T4. *Nature* **227,** 680–685 CrossRef Medline
86. Bradford, M. M. (1976) A rapid and sensitive method for the quantitation of microgram quantities of protein utilizing the principle of protein-dye binding. *Anal. Biochem.* **72,** 248–254 CrossRef Medline
87. Burnette, W. (1981) Western blotting: electrophoretic transfer of proteins from sodium dodecyl sulfate-polyacrylamide gels to unmodified nitrocellulose and radiographic detection with antibody and radioiodinated protein A. *Anal. Biochem.* **112,** 195–203 CrossRef Medline
88. Haid, A., and Suissa, M. (1983) Immunochemical identification of membrane proteins after sodium dodecyl sulfate-polyacrylamide gel electrophoresis. *Methods Enzymol.* **96,** 192–205 CrossRef Medline
89. Boyle, W. J., van der Geer, P., and Hunter, T. (1991) Phosphopeptide mapping and phosphoamino acid analysis by two-dimensional separation on thin-layer cellulose plates. *Methods Enzymol.* **201,** 110–149 CrossRef Medline
90. MacDonald, J. I., and Kent, C. (1994) Identification of phosphorylation sites in rat liver CTP:phosphocholine cytidylyltransferase. *J. Biol. Chem.* **269,** 10529–10537 Medline
91. Morlock, K. R., Lin, Y.-P., and Carman, G. M. (1988) Regulation of phosphatidate phosphatase activity by inositol in *Saccharomyces cerevisiae*. *J. Bacteriol.* **170,** 3561–3566 CrossRef Medline
92. Bligh, E. G., and Dyer, W. J. (1959) A rapid method of total lipid extraction and purification. *Can. J. Biochem. Physiol.* **37,** 911–917 CrossRef Medline
93. Henderson, R. J., and Tocher, D. R. (1992) Thin-layer chromatography: in *Lipid Analysis* (Hamilton, R. J., and Hamilton, S., eds) pp. 65–111, IRL Press, New York
94. Sikorski, R. S., and Hieter, P. (1989) A system of shuttle vectors and yeast host strains designed for efficient manipulation of DNA in *Saccharomyces cerevisiae*. *Genetics* **122,** 19–27 Medline
95. Carman, G. M., and Han, G.-S. (2011) Regulation of phospholipid synthesis in the yeast *Saccharomyces cerevisiae*. *Annu. Rev. Biochem.* **80,** 859–883 CrossRef Medline
96. Henry, S. A., Kohlwein, S. D., and Carman, G. M. (2012) Metabolism and regulation of glycerolipids in the yeast *Saccharomyces cerevisiae*. *Genetics* **190,** 317–349 CrossRef Medline
97. Madera, M., Vogel, C., Kummerfeld, S. K., Chothia, C., and Gough, J. (2004) The SUPERFAMILY database in 2004: additions and improvements. *Nucleic Acids Res.* **32,** D235–D239 CrossRef Medline
98. Koonin, E. V., and Tatusov, R. L. (1994) Computer analysis of bacterial haloacid dehalogenases defines a large superfamily of hydrolases with diverse specificity. Application of an iterative approach to database search. *J. Mol. Biol.* **244,** 125–132 CrossRef Medline
99. Hornbeck, P. V., Zhang, B., Murray, B., Kornhauser, J. M., Latham, V., and Skrzypek, E. (2015) PhosphoSitePlus, 2014: mutations, PTMs and recalibrations. *Nucleic Acids Res.* **43,** D512–D520 CrossRef Medline

Protein kinase C mediates the phosphorylation of the Nem1–Spo7 protein phosphatase complex in yeast

Prabuddha Dey, Wen-Min Su, Mona Mirheydari, Gil-Soo Han and George M. Carman

J. Biol. Chem. 2019, 294:15997-16009.
doi: 10.1074/jbc.RA119.010592 originally published online September 9, 2019
